Fluctuations of topological charges and the CME photon in early RHIC

MORAN JIA[1]

Institute of Particle Physics and Key Laboratory of Quark and Lepton Physics (MOS), CCNU

JULY 19, 2023

[1] Address: jiamr@ccnu.edu.cn

Outline :

- Introduction
- The fluctuations of topological charge and chiral density
- Production of CME photon in early stage
- Summary and Outlook

A picture of Relativistic Heavy Ion Collisions

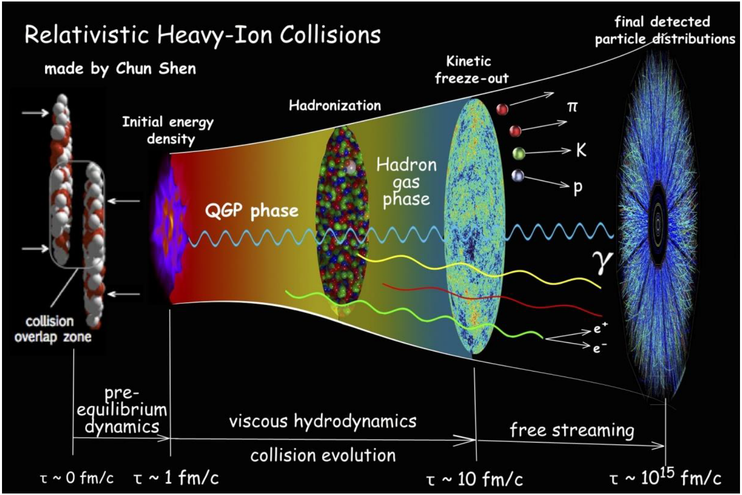

Hints by DIS and RG equations:

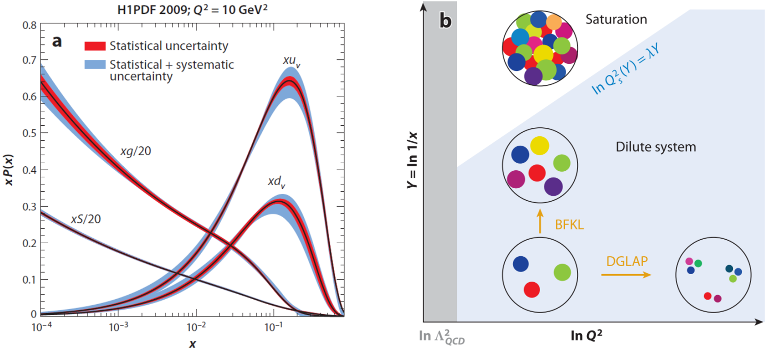

Figure 1: (a) The x evolution of gluon, sea quark, and valence quark distributions (the Lorentz invariant $x \propto \sqrt{Q^2/s}$); (b) Phase diagram for quantum QCD evolution[2].

Key words: High energy collisions, Over occupied gluons.

[2] F. Gelis et al, Rev.Nucl.Part.Sci. 463.60 (2010).

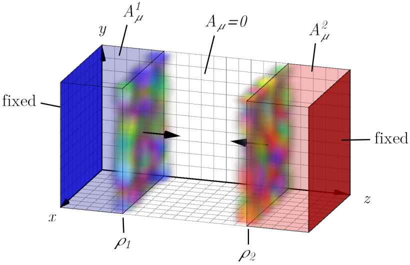

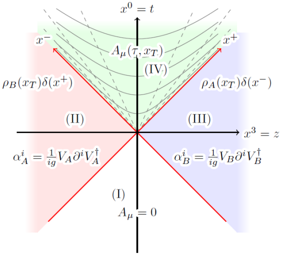

(left) The schematic diagram of the initial conditions in temporal gauge before the collision[3]. (right) The schematic diagram for an ultrarelativistic collision[4].

$$E_\eta = -ig\delta_{ij}\left[\alpha^i_A, \alpha^j_B\right] \qquad B_\eta = -ig\epsilon_{ij}\left[\alpha^i_A, \alpha^j_B\right]$$

[3] D. Gelfand et al, Phys.Rev.D 94, 014020 (2016).
[4] D. Müller, arXiv:1904.04267 [hep-ph].

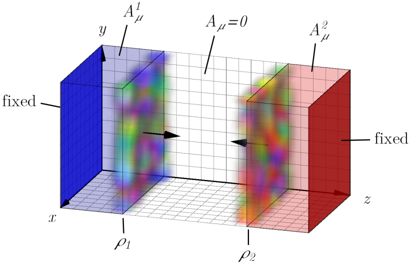

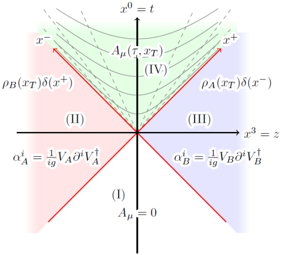

(left) The schematic diagram of the initial conditions in temporal gauge before the collision[3]. (right) The schematic diagram for an ultrarelativistic collision[4].

$$\mathrm{tr}(\mathbf{E} \cdot \mathbf{B}) \neq 0$$

[3] D. Gelfand et al, Phys.Rev.D 94, 014020 (2016).

[4] D. Müller, arXiv:1904.04267 [hep-ph].

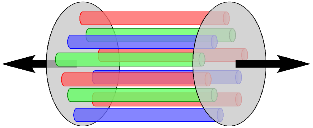

In McLerran-Venugopalan (MV) model[5]:

$$\langle \rho^a(x_T)\rho^b(y_T)\rangle = (g^2\mu)^2\delta^{ab}\delta^2(x_T - y_T), \tag{1}$$

and the observables can be computed by

$$\langle \mathcal{O}\left[\mathcal{A}_\mu\right]\rangle_\Lambda = \int D\rho W_\Lambda[\rho]\mathcal{O}\left[\mathcal{A}_\mu\right] \tag{2}$$

[5] $Q_s/g^2\mu$ is studied in: T. Lappi, Eur.Phys.J.C 55,285 (2008).

The topological fluctuations in early evolution

The Adler-Bell-Jackiw anomaly equation[6]

$$\partial_\mu j_5^\mu = 2 \sum_{flavor} m_q \bar{q} i \gamma_5 q - \frac{N_f}{16\pi^2} F^a_{\mu\nu} \tilde{F}^{a,\mu\nu}. \tag{3}$$

An approach in early stage in (τ, η) coordinates:

$$(\partial_\tau + \frac{1}{\tau}) j_5^\tau = -\frac{N_f}{16\pi^2} F^a_{\mu\nu} \tilde{F}^{a,\mu\nu} = \frac{N_f}{8\pi^2} \mathrm{tr}(\mathbf{E} \cdot \mathbf{B}) \tag{4}$$

Notes: The r.h.s. of the above equation is just a (local) variation of (global) topological invariant, which is also know as ΔN_{CS}.

[6] for each flavor $j_5^\mu = \bar{q}\gamma^\mu\gamma_5 q$.

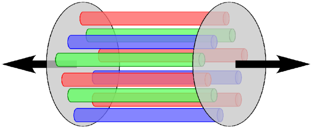

The variation of CS number:

$$\Delta N_{CS} = \rho = \frac{1}{8\pi^2}\mathrm{tr}(\mathbf{E}\cdot\mathbf{B}). \qquad (5)$$

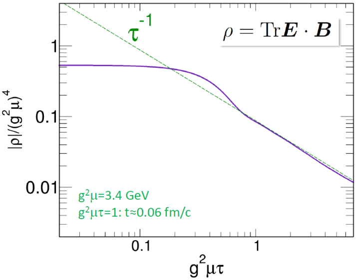

Figure 2: Longitudinal expansion of $|\rho|$.

By solving Eq.(4), for each flavor:

$$\tau j_5^\tau(\tau, x_\perp) = \frac{1}{8\pi^2}\int_0^\tau d\tau'\tau'\mathrm{tr}(\mathbf{E}\cdot\mathbf{B}) \qquad (6)$$

Evolution of the fluctuations:

Chiral density per rapidity,

$$\langle n_5^2(\tau, x_\perp)\rangle = \langle j_5^\tau(\tau, x_\perp)^2\rangle \quad (7)$$

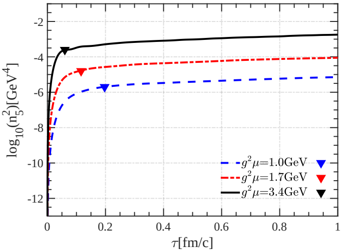

Figure 3: Fluctuations of chiral density as a function of proper time[7].

Correlator of the chiral density:

We define the correlator as:

$$D(|x_\perp|/\lambda_5) \propto \langle n_5(0)n_5(|x_\perp|)\rangle, \quad (8)$$

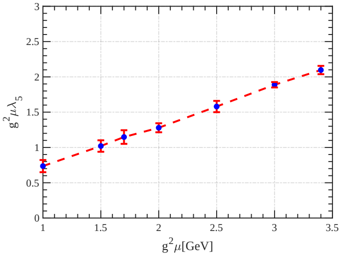

Figure 4: Correlation length of chiral density at different scales[7].

[7] MRJ et al, Phys.Rev.D 103, 014026 (2021).

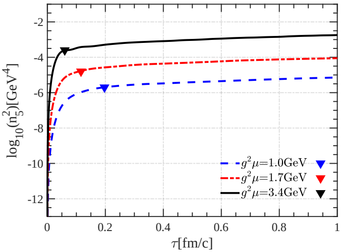

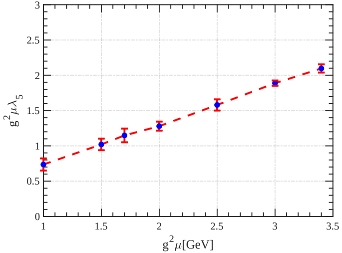

Comments:

- Formation time is order of $\mathcal{O}(1/g^2\mu)$.
- Correlation length of chiral density $\mathcal{O}(1/g^2\mu)$.

$$\frac{\langle N_5^2 \rangle}{V^2} = \frac{\langle n_5^2 \rangle}{\tau^2} \tag{9}$$

The estimation, e.g. $\sqrt{\langle N_5^2 \rangle / V^2} \approx 6.48\mathrm{fm}^{-3}$ at $g^2\mu = 3.4\mathrm{GeV}$, is pretty large.

Some ingredients for application to CME:

- Chiral medium generated by fluctuations of glasma field.
- Strong magnetic field produced by fast moving charged particles.

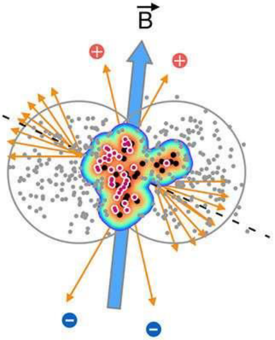

The chiral chemical potential:

In massless limit and early stage approach (n_5 as per unit volume below):

$$n_5 = \frac{\mu_5^3}{3\pi^2} + \frac{\mu_5}{3}\left(T^2 + \frac{\mu^2}{\pi^2}\right) \xrightarrow[\mathit{Stage}]{\mathit{Early}} n_5 \approx \frac{\mu_5^3}{3\pi^2}. \tag{10}$$

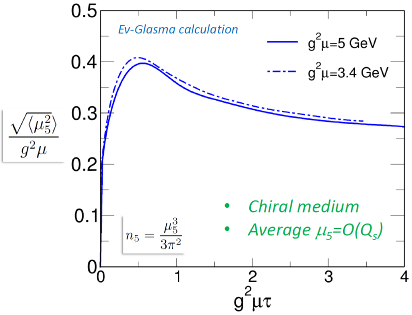

Figure 5: Scaling property of the chiral chemical potential.

An ansatz of μ_5-correlator[8]:

$$\langle \mu_5(\tau_1, x_T)\mu_5(\tau_2, y_T)\rangle = \left\langle \mu_5^2\left(\frac{\tau_1+\tau_2}{2}\right)\right\rangle (2\lambda_\tau)\delta(\tau_1-\tau_2) \times \frac{|x_T-y_T|}{\lambda_5} K_1\left(\frac{|x_T-y_T|}{\lambda_5}\right) \tag{11}$$

Notes:

- The correlator is proportional to $\langle \mu_5^2 \rangle$.
- λ_5 is the correlation length mentioned above.
- λ_τ balances the dimension of $\delta(\tau_1-\tau_2)$, and $\lambda_\tau \ll \lambda_5$.

[8] Constructed through our full numerical computation.

The strong magnetic field:

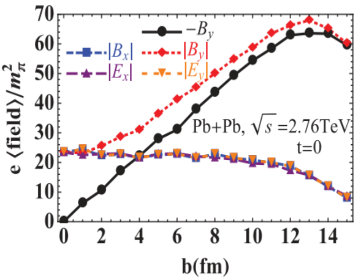

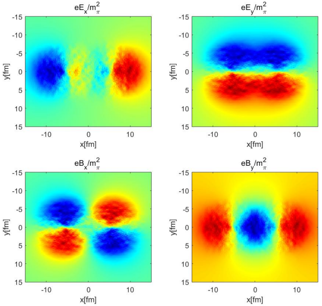

(left)[9] The electromagnetic fields as functions of the impact parameter b; (right)[10] The configuration of electromagnetic fields at $\tau = 0$ with $\mathrm{b} = 8\mathrm{fm/c}$.

$$\vec{B} \approx B_y; \qquad \vec{E} \approx 0. \tag{12}$$

[8] W.T. Deng, X.G. Huang, Phys.Rev.C 85, 044907 (2012).

[9] Same strategy as in A. Bzdak, V. Skokov, Phys.Lett.B. 710.171 (2012)

The strong magnetic field:

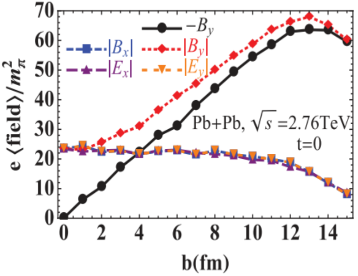

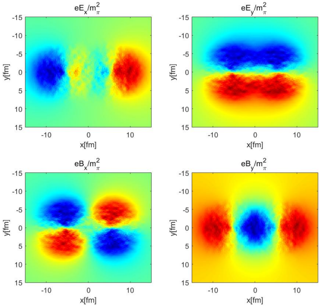

(left)[9] The electromagnetic fields as functions of the impact parameter b; (right)[10] The configuration of electromagnetic fields at $\tau = 0$ with $\mathrm{b} = 8\mathrm{fm/c}$.

$$B_y(\tau, \eta) = \langle B_0 \rangle f(\tau) \cosh \eta \quad \text{with} \quad f(\tau) = \frac{1}{1 + \tau^2/\tau_B^2} \tag{13}$$

[8] W.T. Deng, X.G. Huang, Phys.Rev.C 85, 044907 (2012).

[9] Same strategy as in A. Bzdak, V. Skokov, Phys.Lett.B. 710.171 (2012)

The Photons from Chiral Anomaly processes:

(Note: also another interesting talk of axion-photon by G. Endrödi, morning 16th.)

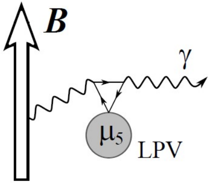

Figure 6: Schematic figure for the single photon production as a consequence of the axial anomaly and the external magnetic field[11].

$$\mathcal{L}_P = \frac{N_c e^2 \mathrm{Tr}(\mathrm{Q}^2)}{8N_f\pi^2}\epsilon^{\mu\nu\rho\sigma}\mathcal{A}_\mu[\bar{F}_{\nu\rho} + \partial_\nu\mathcal{A}_\rho]\partial_\sigma\theta \tag{14}$$

[11] K. Fukushima, K. Mameda, Phys.Rev.D. 86.071501 (2012).

Spectrum of the photon can be written as:

$$q_0 \frac{dN_\gamma}{dq^3} \propto \left| (1 - \frac{q_x^2}{q^2})\zeta_x^2(q) + (1 - \frac{q_y^2}{q^2})\zeta_y^2(q) - \frac{2q_x q_y}{q^2}\zeta_x(q)\zeta_y(q) \right| \quad (15)$$

where,

$$\zeta_i(q) \equiv \int d^4x e^{-iq\cdot x} eB_i(x)\mu_5(x), \quad i = x, y. \quad (16)$$

Then, Eq.(12) can be further simplified:

$$\frac{dN_\gamma}{2\pi q_T dq_T dy} = \alpha_e \left(\frac{N_c \mathrm{tr}(\mathrm{Q}^2)}{4\pi^3} \right)^2 (1 - \frac{q_y^2}{q^2}) \langle |\zeta_y^2(q)| \rangle, \quad (17)$$

the spectrum of photon can be computed with help of μ_5-correlator.

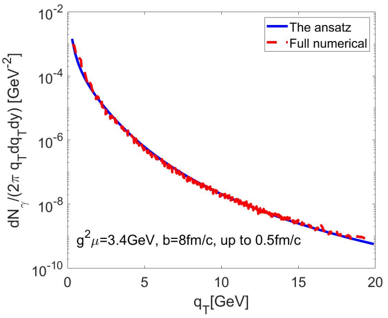

Figure 7: The CME photon spectrum, $y = 0$ and $\tau_B = 0.1\mathrm{fm/c}$[12].

From analysis based on the ansatz, we can read off v_2 from Eq.(14) directly:

$$1 - \frac{q_y^2}{q^2} = \cos^2\phi = \frac{1+\cos 2\phi}{2} \rightarrow v_2 = \frac{1}{2}. \tag{18}$$

[12] The paper work will be available online soon.

Summary

- Fluctuation of chiral density is large in early stage, which induces the chiral imbalance. (see similar talk of A. Huang, morning 16th)
- The typical scale of the chiral density is closely related to the saturation momentum.
- The photon through chiral anomaly process is computed.

Outlook:

- Since the glasma simulation also provide large chiral fluctuations, it would be another meaningful input for Hydro-evolution.
- It will be more interesting to make further improvements as well as other applications on the ansatz of μ_5-correlator.

Comment:

- A possible probe of CME and/or potential candidate to solve 'direct photon puzzle'?

Thanks for your attention!

Collaborators:

- M. Ruggieri, J.H. Liu, L. Oliva, K. Fukushima, X.G. Huang, H.F. Zhang

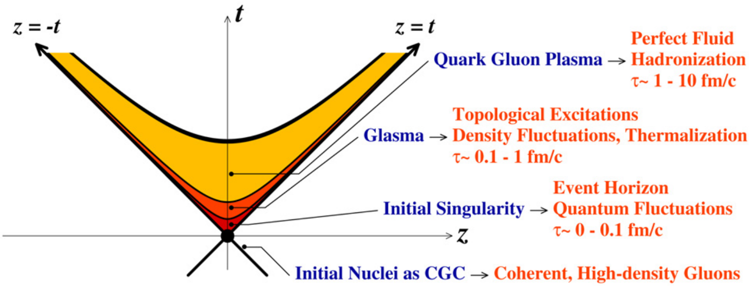

Figure 8: Light cone diagram illustrating the evolution of matter produced in heavy ion collisions[13].

[13] K. Fukushima et al, Nucl. Phys.A 786.107 (2007)

Working with Fock-Schwinger gauge $x^+A^- + x^-A^+ = 0$, the action:

$$S = \frac{1}{2}\int d^4x \mathrm{tr}\left[\mathrm{F}_{\mu\nu}\mathrm{F}^{\mu\nu}\right], \tag{19}$$

the canonical momenta are given by

$$E_i = \tau\partial_\tau A_i, \tag{20}$$

$$E_\eta = \frac{1}{\tau}\partial_\tau A_\eta. \tag{21}$$

As a consequence, the Hamiltonian density can be read as

$$\mathcal{H} = \mathrm{tr}\left[\frac{1}{\tau}\mathrm{E}_\mathrm{i}^2 + \tau\mathrm{E}_\eta^2 + \frac{1}{\tau}\mathrm{F}_{\eta\mathrm{i}}^2 + \frac{\tau}{2}\mathrm{F}_\mathrm{ij}^2\right]. \tag{22}$$

The CYM equations can be solved via

$$\partial_\tau E_i = \frac{1}{\tau}\mathcal{D}_\eta F_{\eta i} + \tau\mathcal{D}_j F_{ji}, \tag{23}$$

$$\partial_\tau E_\eta = \frac{1}{\tau}\mathcal{D}_j F_{j\eta}. \tag{24}$$

Liénard-Wiechert Potentials:

$$e\vec{E} = \alpha_e \sum_n \frac{(1-v^2)\vec{R}}{R^3(1-[\vec{R}\times\vec{v}]^2/R^2)^{3/2}} \quad (25)$$

$$e\vec{B} = \alpha_e \sum_n \frac{(1-v^2)\vec{v}\times\vec{R}}{R^3(1-[\vec{R}\times\vec{v}]^2/R^2)^{3/2}} \quad (26)$$

The Woods-Saxon distribution[14]:

$$\rho(r) = \rho_0(1+\omega\frac{r^2}{r_0^2})(1+e^{\frac{r-r_0}{a}})^{-1}. \quad (27)$$

$b \approx 8fm$ in Pb-Pb@LHC $\Rightarrow$

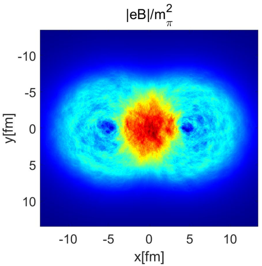

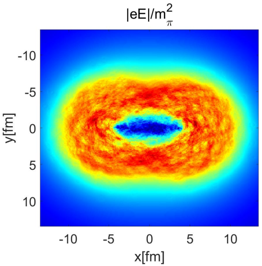

[14] B. Alver, et al, arXiv:0805.4411 [nucl-ex].

Computation of the spectrum with ansatz μ_5-correlator:

Working in (τ, η) frame:

$$\zeta_i(q)\Big|_{y=0} = \int d\tau d\eta \tau e^{-iq_T \tau \cosh\eta} \int d^2 x_T e^{iq_T \cdot x_T} eB_i(\tau, x_T, \eta)\mu_5(\tau, x_T), \quad (28)$$

by using the ansatz with the following definition

$$\mathcal{J}(q_T) = 4 \int \tau^2 d\tau f(\tau)^2 \left\langle \mu_5^2(\tau) \right\rangle |K_1(iq_T\tau)^2|, \quad (29)$$

the spectrum reads:

$$\frac{dN_\gamma}{q_T dq_T dy}\Big|_{y=0} = \frac{1}{2}\alpha_e \left(\frac{N_c \mathrm{Tr}(Q^2)}{4\pi^3}\right)^2 \left[\frac{4\pi\lambda_5^2}{(1+q_T^2\lambda_5^2)^2}\right] (2\lambda_\tau)(eB_0)^2 A_T \mathcal{J}(q_T) \quad (30)$$

where A_T is the transverse area.

Comparison with other direct photon sources:

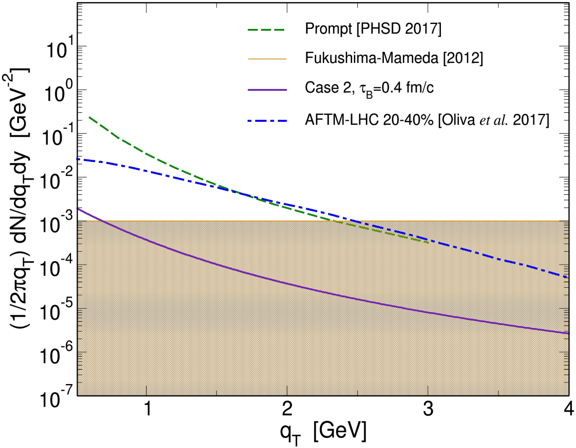

The elliptic flow of CME photon:

The Fourier expansion:

$$q_0 \frac{dN_\gamma}{dq^3} = \frac{1}{2\pi} \frac{dN_\gamma}{q_T dq_T dy} \left(1 + 2 \sum_{n=1}^{\infty} v_n \cos\left[n(\phi - \psi_{RP}) \right] \right), \tag{31}$$

we choose $\psi_{RP} = 0$, and full numerical check of the elliptic flow:

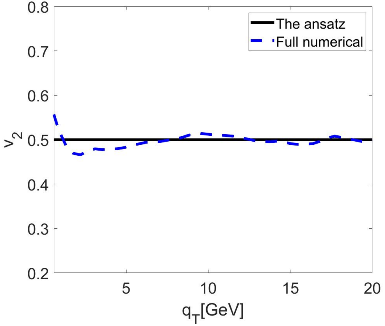

Besides the CME photon, a potential candidate to solve 'direct photon puzzle'?

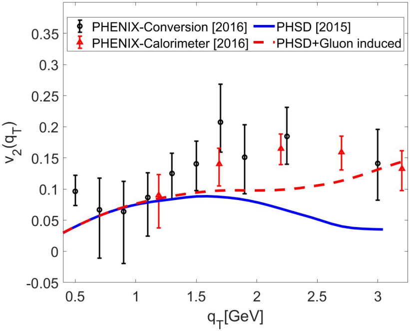

Figure 9: The PHENIX measurement[15] and associated v_2 improvement on top of PHSD[16] prediction. Photon magnetic induced gluon fusion and splitting in early stage[17].

[15] A. Adare, et al, (PHENIX), Phys.Rev.C 94.064901(2016).

[16] O. Linnyk, et al, Phys.Rev.C 92.054914 (2015).

[17] MRJ, Huixia Li, Defu Hou, arXiv:2211.16770 [hep-ph].